

# Retinal Ganglion Cell Loss in a Rat Ocular Hypertension Model Is Sectorial and Involves Early Optic Nerve Axon Loss

Ileana Soto,<sup>1</sup> Mary E. Pease,<sup>2</sup> Janice L. Son,<sup>3</sup> Xiaobai Shi,<sup>1</sup> Harry A. Quigley,<sup>2</sup> and Nicholas Marsh-Armstrong<sup>1,2,3</sup>

**PURPOSE.** Previous analyses of the DBA/2J mouse glaucoma model show a sectorial degeneration pattern suggestive of an optic nerve head insult. In addition, there are large numbers of retinal ganglion cells (RGCs) that cannot be retrogradely labeled but maintain RGC gene expression, and many of these have somatic phosphorylated neurofilament labeling. Here the authors further elucidate these features of glaucomatous degeneration in a rat ocular hypertension model.

**METHODS.** IOP was elevated in Wistar rats by translimbal laser photocoagulation. Retina whole mounts were analyzed for Sncg mRNA in situ hybridization, fluorogold (FG) retrograde labeling, and immunohistochemistry for phosphorylated neurofilaments (pNF) at 10 and 29 days after IOP increase. A novel automatic method was used to estimate axon numbers in plastic sections of optic nerves.

**RESULTS.** Sncg mRNA was confirmed as a specific marker for RGCs in rat. Loss of RGCs after IOP elevation occurred in sectorial patterns. Sectors amid degeneration contained RGCs that were likely disconnected because these had pNF in their somas and dendrites, were not labeled by FG, and were associated with reactive plasticity within the retina. Most of the axon loss within the optic nerve already occurred by 10 days after the onset of IOP elevation.

**CONCLUSIONS.** These data demonstrate that the pattern of RGC loss after laser-induced ocular hypertension in rats is similar to that previously reported in DBA/2J mice. The results support the view that in glaucoma RGC axons are damaged at the optic nerve head and degenerate within the optic nerve before there is loss of RGC somas. (*Invest Ophthalmol Vis Sci.* 2011;52:434-441) DOI:10.1167/iovs.10-5856

We recently showed that RGC degeneration in DBA/2J mice is sectorial and that within the sectors of degeneration there are many RGCs that maintain gene expression after

they can no longer be retrogradely labeled from the superior colliculus.<sup>1</sup> Among these putatively disconnected RGCs, many have accumulation of phosphorylated neurofilaments (pNF) in their somas and dendrites, a cellular redistribution observed in RGCs after severe axonal injuries.<sup>2-4</sup> However, given that some have argued that the DBA/2J mouse model does not recapitulate nonpigmentary glaucoma, an important priority was to determine whether key neuropathologic features observed in DBA/2J are conserved in other animal models of glaucoma. In addition, because RGC degeneration is asynchronous and related to aging in DBA/2J, more acute animal models may be preferable for establishing the sequence of progressive changes in glaucoma.

Two popular rat glaucoma animal models, increasing IOP by injection of hypertonic saline into episcleral vessels<sup>5</sup> or laser injury to aqueous humor outflow channels,<sup>6,7</sup> produce degenerations that are generally similar in extent, pattern, and mechanism.<sup>8</sup> Although the IOP increase observed in these models is more acute and generally higher than in typical human open angle glaucoma, the degeneration is faster and more synchronous than in DBA/2J mice. Here, we use one such model to confirm and further investigate the chronology of several neuropathologic features first described in DBA/2J mice.

## METHODS

### Animals

Experiments were performed on female Wistar rats, each weighing 550 to 650 g, using procedures in accordance with the ARVO Statement for the Use of Animals in Ophthalmic and Vision Research. Rats were housed in a 14-hour light/10-hour dark cycle and had food and water ad libitum.

### Translimbal Laser Photocoagulation

IOP was increased unilaterally in rats as previously described.<sup>6</sup> A 532-nm diode laser (Coherent Radiation, Clement-Ferrand, France) was used to scar the trabecular meshwork and perilimbal veins, delivering 45 to 50 spots of 50- $\mu$ m size, 600-mW power, and 0.6-second duration. IOP of lasered and nonlasered control eyes were monitored in anesthetized rats using a rebound tonometer (TonoLab; Colonial Medical Supply, Franconia, NH). Two groups of rats were treated. The first group involved eight rats and was analyzed 29 days after lasering by retrograde labeling and by molecular markers, together with five control rats. The second group involved 18 rats that were analyzed only by molecular markers, half each at 10 days and 29 days after lasering.

### Retrograde Tracing, Whole Mount Retina In Situ Hybridization, and Antibody Labeling

RGCs were labeled by injection of fluorogold (FG; Fluorochrome, Inc., Denver, CO) into both superior colliculi 3 days before euthana-

From the <sup>1</sup>The Solomon H. Snyder Department of Neuroscience and the <sup>2</sup>Department of Ophthalmology, Johns Hopkins University School of Medicine, Baltimore, Maryland; and the <sup>3</sup>Hugo W. Moser Research Center, Kennedy Krieger Institute, Baltimore, Maryland.

Supported by a Glaucoma Research Foundation Catalyst for a Cure research grant (NM-A); National Eye Institute Postdoctoral Fellowship Grant 5T32 EY07143-12 (IS); a Johns Hopkins University Provost's Undergraduate Research Award (JLS); and National Eye Institute Grants RO1 EY02120 and EY01765 (HAQ).

Submitted for publication May 10, 2010; revised June 24 and July 16, 2010; accepted August 2, 2010.

Disclosure: I. Soto, None; M.E. Pease, None; J.L. Son, None; X. Shi, None; H.A. Quigley, None; N. Marsh-Armstrong, None

Corresponding author: Nicholas Marsh-Armstrong, Hugo W. Moser Research Center, Kennedy Krieger Institute, Baltimore, MD 21205; marsh-armstrong@kennedykrieger.org.

tizing as previously described.<sup>9</sup> RGCs were identified in whole mount retinas using in situ hybridization for *Sncg* mRNA essentially as previously reported in mice.<sup>1</sup> A cDNA of rat *Sncg* (UI-R-CW0-BV-08-08-0-UI; Open Biosystems, Huntsville, AL) was used to generate a digoxigenin-labeled antisense riboprobe, which was then hydrolyzed. The in situ hybridization signal was detected using a Cy-3 tyramide substrate (Perkin Elmer, Boston, MA). After in situ hybridization, retinas were incubated for 3 nights in 2F11 antibody (Dako Cytomation, Carpinteria, CA), which recognizes phosphorylated forms of 68 kDa and 200 kDa neurofilaments or an antibody to FG (Chemicon International, Temecula, CA); nuclei were detected as previously described.<sup>1</sup>

### RGC Counts in Retinal Whole Mounts

Automatic counts of cells containing *Sncg* mRNA or FG were obtained from rat retinas essentially as previously described for mouse retinas.<sup>1</sup> The identification of RGCs was based on segmentation criteria that identified an expected number of RGCs in control retinas, approximately 100,000. Counts of pNF+ RGCs and their classification into weak or strong subtype were carried out as described previously.<sup>1</sup> In addition, 2 × 2-mm regions of retinas were imaged again as nonoverlapping frames, each 50 z-sections 0.4 μm apart, using a confocal microscope (Fluoview FV1000; Olympus, Tokyo, Japan). Image visualization software (Imaris 6.3; Bit-

plane Inc. St. Paul, MN) was used for automatic volume rendering and manual tracing of individual axons.

### Estimation of Axon Number

One-micrometer plastic cross-sections of optic nerve obtained approximately 1.5 mm behind the globe were stained with toluidine blue. Axon counts were obtained by two methods. The first, referred to as the semiautomatic method, was that used in previous reports.<sup>9,10</sup> For the automatic method, nerve cross-sections were imaged in their entirety as nonoverlapping frames using a 100 × 1.4 NA objective and imaging software-driven autofocusing (IPLab; Becton Dickinson, Franklin Lakes, NJ). Mosaics of these images were used to manually trace nerve outlines. Axons were identified as small clear objects in both an unprocessed mosaic and a mosaic subjected to an imaging software (IPLab; Becton Dickinson) rolling-ball local background subtraction. Size criteria were used to exclude intervening glia. The intensity mean ± SD of the intervening glia was used as minimum value filters to exclude objects such as myelin debris and highly degenerated axons. Variables were optimized so that they would find the expected number of axons in five calibration optic nerves, used in the training of new users of the semiautomatic axon counting method (0%–75% degeneration). For validation purposes, a set of five nerves of the present study (different from the training optic nerves; data not shown) and 30 nerves from a different study<sup>10</sup> were counted by both the automatic and semiautomatic methods.

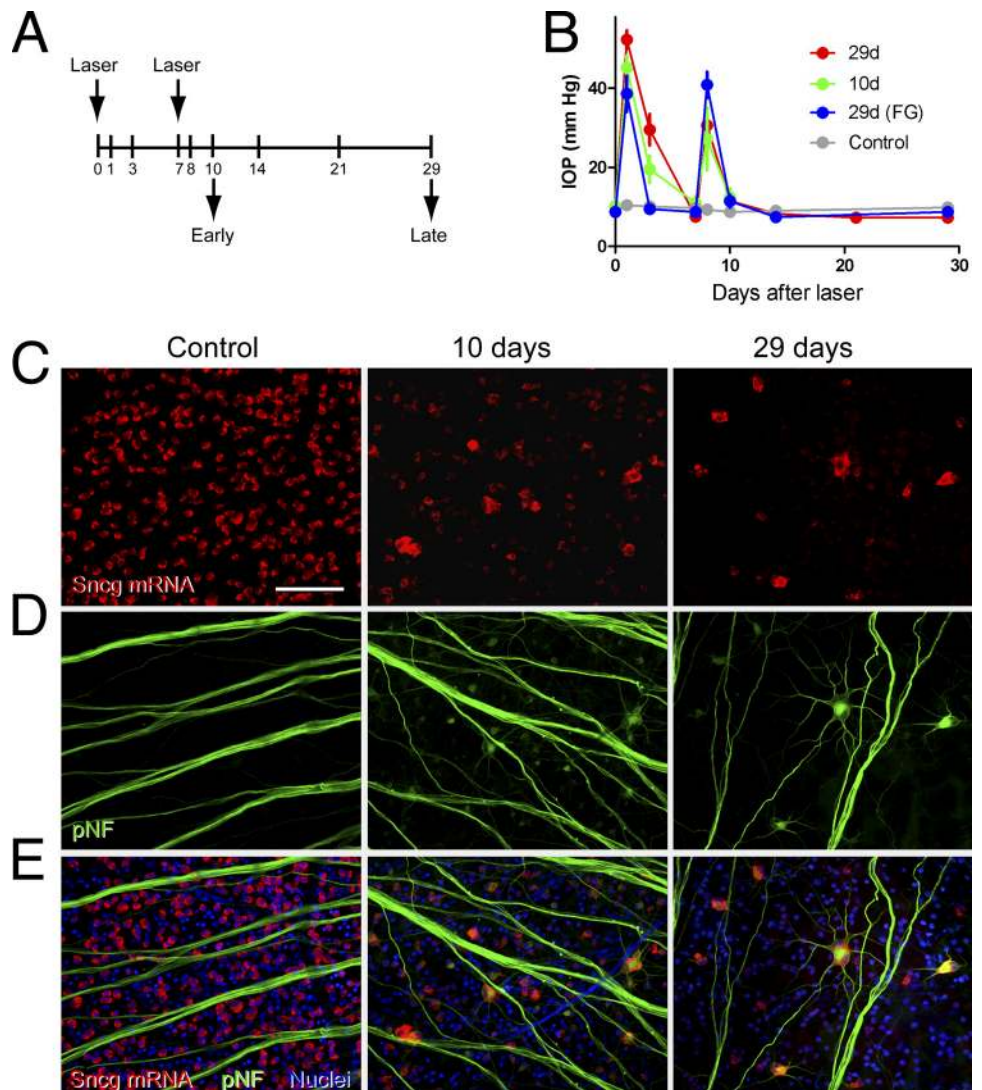


**FIGURE 1.** Translimbal laser photocoagulation increases IOP and leads to RGC degeneration that involves loss of *Sncg*-expressing cells, decreases in *Sncg* mRNA gene expression in most RGCs, and the appearance of somatic pNF in many RGCs. **(A)** Experimental design shows timeline of lasering (arrows above timeline), IOP measurements (ticks), and analyses (arrows below timeline). **(B)** IOPs (mean ± SEM) recorded in the rats used in the present study. Red and green values represent IOP from lasered eyes of rats analyzed with molecular markers only at 10 and 29 days, respectively. Blue values represent IOPs of lasered eyes from rats analyzed at 29 days by both FG labeling and molecular markers. Gray values represent the IOP of nonlasered eyes of rats labeled with FG and analyzed at 29 days. IOP from the other nonlasered groups are not shown but were similar. Retinal whole mount views labeled for *Sncg* mRNA (C), pNF (D), and merged views of both, together with nuclear labeling (E), show that at 10 days there is decreased gene expression in and loss of many RGCs and that by 29 days after lasering the density of RGCs is dramatically decreased, whereas many remaining RGCs show a redistribution of pNF in a somatodendritic rather than an axon-only pattern. Scale bar, 50 μm.



## RESULTS

### RGC Degeneration after Ocular Hypertension Involves Loss of Sncg-Expressing Cells and Redistribution of Phosphorylated Neurofilaments within Remaining RGCs

Retinas of Wistar rats were examined 10 and 29 days after the first of two sessions of translimbal laser photocoagulation (Fig. 1A). This laser regimen produced IOP spikes peaking the day after each of the laser sessions (Fig. 1B). In whole mount preparations of retinas that were not lasered, Sncg mRNA labeled numerous cell somas, and an antibody against pNF labeled only axons (Figs. 1C-E, left). By 10 days after laser, retinas had fewer cells labeled by Sncg mRNA (Figs. 1C-E, middle). Relative to control retinas, the level of Sncg mRNA per cell was also decreased in most cells. In addition, by 10 days after laser, pNF immunoreactivity was found not only in axons but also weakly in the somas of many Sncg+ cells (weak pNF+ RGCs) and strongly in somas and dendrites of some others (strong pNF+ RGCs). By 29 days (Figs. 1C-E, right), there were fewer Sncg+ cells, and though some had very low levels of Sncg mRNA expression, others had Sncg mRNA levels higher than in RGCs of control retinas (Fig. 1C). Compared with retinas at 10 days, those at 29 days had fewer of the weak pNF+ RGCs (Fig. 1D). Paradoxically, at both 10 and 29 days, the highest levels of Sncg mRNA expression were observed in the RGCs with strong pNF labeling (Fig. 1E; see Fig. 4A).

To ascertain the extent of RGC loss, retinal whole mounts processed for in situ hybridization of Sncg and immunohisto-

chemistry for pNF were imaged at 20 $\times$  magnification and were used to generate mosaic composites of the retina surface (Fig. 2A). Control retinas (e.g., Fig. 2A, left) showed a relatively uniform density of Sncg+ cells throughout and had few or no pNF+ RGCs. By 10 days after laser (e.g., Fig. 2A, middle), retinas had areas with reduced Sncg+ cell density, alternating with areas of normal or near normal density. These same retinas had many pNF+ RGCs, and most of these were of the weak variety (green dots) with far fewer of the strong variety (red dots). By 29 days after laser (e.g., Fig. 2A, right), the density of Sncg+ cells was lower than by 10 days, though some retinas had sectors that retained relatively higher densities. By 29 days, there were also large numbers of pNF+ RGCs, and most of these were of the strong variety with far fewer of the weak variety. Indeed, there was a consistent large difference in proportions of weak and strong pNF+ RGCs between 10 and 29 days (Fig. 2B;  $P < 0.0001$ , *t*-test): 3.8%  $\pm$  1.7% of the pNF+ RGCs were of the strong variety at 10 days ( $n = 3$ ) and 85.9%  $\pm$  2% were of the strong variety at 29 days ( $n = 3$ ). Based on automatic counts of Sncg-labeled objects (Figs. 2C, 2D), laser significantly decreased ( $P < 0.0001$ , one-way ANOVA) the number of RGCs. The number of Sncg+ cells was 100,318  $\pm$  5,601 in control retinas ( $n = 3$ ), decreased ( $P < 0.05$ , Tukey's multiple comparison test) to 68,807  $\pm$  15,804 by 10 days ( $n = 4$ ) and decreased even further ( $P < 0.01$ , Tukey's multiple comparison test) to 13,947  $\pm$  4,233 by 29 days ( $n = 4$ ). The total number of pNF+ RGCs (weak plus strong) per retina was 2  $\pm$  3 in control retinas, 5,142  $\pm$  1,298 at 10 days, and 1,682  $\pm$  436 at 29 days after laser (Fig. 2C). Thus, laser produced a significant increase in the number of

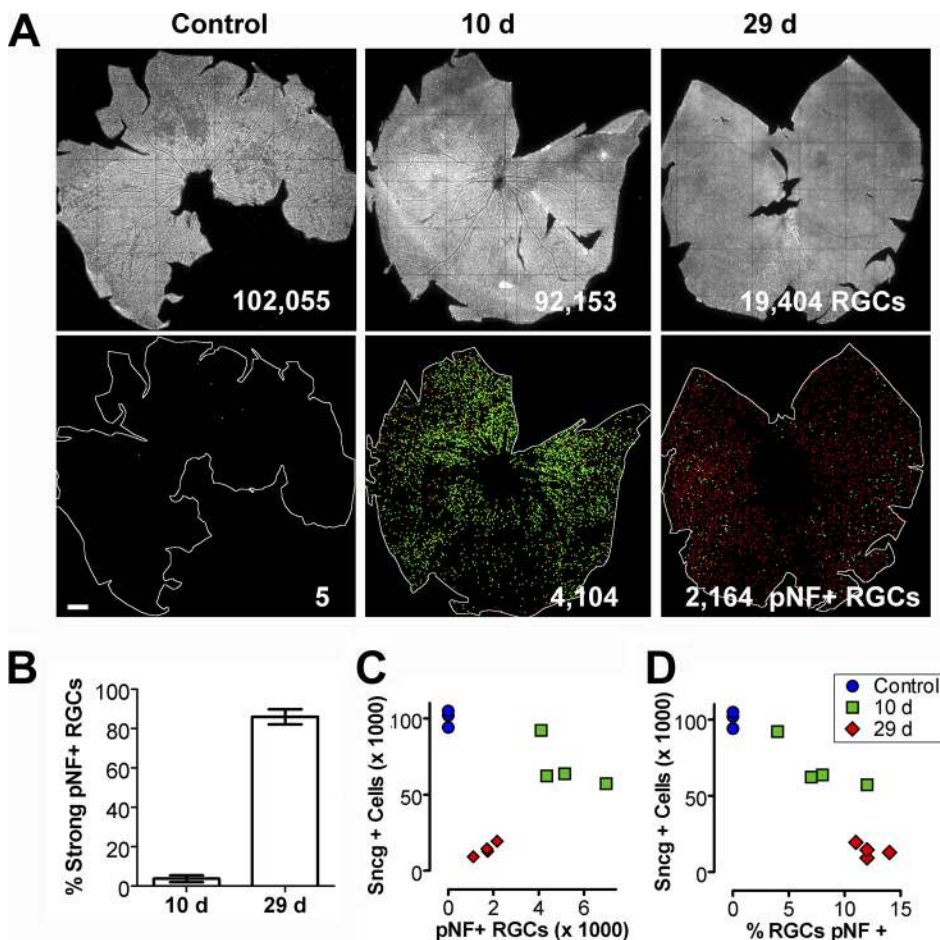


**FIGURE 2.** Increased number and different types of RGCs with somatic phosphorylated neurofilaments at 10 and 29 days after laser. (A) Sncg mRNA reveals loss of RGCs after laser, and pNF+ RGC positions in the same retinas show large numbers of pNF+ RGCs in degenerating regions. Most of the pNF+ RGCs are of the weak variety (green dots) at 10 days and of the strong variety (red dots) at 29 days after laser. (B) The percentage of pNF+ RGCs that are of the strong variety significantly increased between 10 and 29 days after laser. (C) The number of pNF+ RGCs (weak and strong together) plotted relative to the number of remaining RGCs (Sncg mRNA + cells) showed significant loss of RGCs at 10 and 29 days after laser and thousands of pNF+ RGCs at both 10 and 29 days. (D) Replotting the same data of C in terms of the percentage of Sncg+ cells that are pNF+ shows that the fraction of RGCs that were pNF+ is highest 29 days after laser. Scale bar, 1 mm.

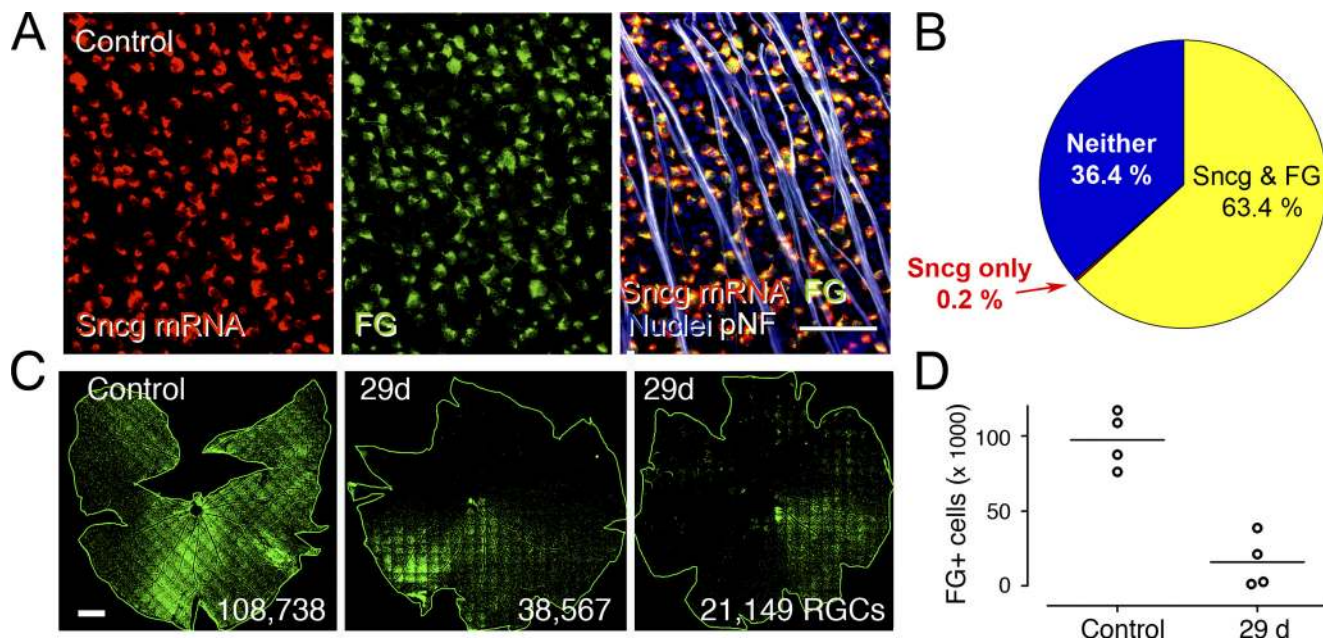


**FIGURE 3.** Retrograde FG labels the same cells as Sncg mRNA and reveals RGC sectorial degeneration. (A) The same cells are labeled by Sncg mRNA (red) and FG (green) in control retinas. (B) More than half the cells in the retinal ganglion cell layer of control retinas are RGCs, labeled by both Sncg mRNA and FG. (C) FG labeling in a control retina and two retinas 29 days after lasering shows that translimbal laser photocoagulation produces sectorial degeneration patterns. (D) Numbers of RGCs labeled by FG are significantly reduced 29 days after lasering. Scale bars: 50  $\mu$ m (A); 1 mm (C).

pNF+ RGCs ( $P < 0.0001$ , one-way ANOVA), which was highest 10 days after lasering. Based on the counts of Sncg+ cells and pNF+ RGCs, the percentage of remaining RGCs with somatic pNF was  $0.001 \pm 0.002$  in control retinas,  $8 \pm 3$  at 10 days, and  $12 \pm 1$  at 29 days after lasering (Fig. 2D). Thus, lasering also produced a significant ( $P < 0.001$ , one-way ANOVA) increase in the percentage of RGCs with somatic pNF that was highest at 29 days.

### Degeneration Occurs in Sectors Containing RGCs That Cannot Be Retrogradely Labeled from the Superior Colliculus

Although data show the Sncg is expressed in RGCs of multiple species, including in cells coexpressing Brn3 in rat retina primary cell cultures,<sup>11</sup> additional experiments are needed to confirm that Sncg mRNA can be used as a selective marker for RGCs in the rat, as previously shown in the mouse.<sup>1</sup> To demonstrate this, retinas were labeled by FG injection into the superior colliculus, and the extent of colocalization between FG and Sncg mRNA was analyzed. Inspection of high-power views of such retinas (Fig. 3A) revealed that cells that were FG labeled also expressed Sncg mRNA, and vice versa. Manual counts from midperipheral fields of retinas (four 20 $\times$  fields per retina in each of four retinas, for a total of 7985 cells) revealed that  $63.4\% \pm 3.2\%$  of nuclei in the ganglion cell layer were surrounded by both Sncg mRNA and FG,  $0.2\% \pm 0.3\%$  expressed Sncg mRNA but were not labeled by FG, and  $0.0\% \pm 0.1\%$  were labeled by FG alone;  $36.4\% \pm 3.0\%$  of nuclei were surrounded by neither Sncg mRNA nor FG and likely represented mainly amacrine cells (Fig. 3B). Thus, Sncg mRNA is a selective marker for RGCs in intact retinas of rats.

Retinas from a second set of rats that had been lasered 29 days before and that also had similar increases in IOP (Fig. 1B) were compared with control retinas by FG retrograde labeling. In the retinas of lasered eyes, there were large pie-shaped sectors lacking FG (Fig. 3C). Such sectorial degeneration was evident in 3 of 4 lasered retinas labeled by FG (data not

shown). Similar sectors of degeneration were also evident in 6 of 8 retinas labeled by Sncg mRNA but not FG (Fig. 2 and Supplementary Fig. S1, <http://www.iovs.org/lookup/suppl/doi:10.1167/iovs.10-5856/-/DCSupplemental>). Degeneration was uniform only in the most severely affected retinas. Based on automatic counts of FG-labeled objects in this second set of lasered rats, control retinas had  $97,323 \pm 18,862$  FG + cells, and retinas 29 days after lasering had  $15,955 \pm 17,568$  FG + cells (Fig. 3D); thus, lasering produced a large loss of cells labeled by FG ( $P < 0.001$ , one-tailed unpaired *t*-test).

In the retinas of lasered eyes, FG and Sncg mRNA were generally found in the same cells (Fig. 4A). However, in the fields with reduced numbers of RGCs, there were also many Sncg+ cells that were not retrogradely labeled, and many of these were the pNF+ RGCs. To determine the fraction of Sncg+ cells that were not retrogradely labeled and the fraction of these that had somatic pNF, cells were counted in 20 $\times$  magnification fields of retinas from control (2028 cells in 8 fields from 4 retinas) and lasered (2006 cells in 52 fields from 4 retinas) eyes. Fields were divided into those that were non-degenerating if they had near normal densities of Sncg+ cells and no pNF+ RGCs, mildly degenerating if they had near normal densities of Sncg+ cells but several pNF+ RGCs, or severely degenerating if they had reduced densities of Sncg+ cells and numerous pNF+ RGCs. Essentially all Sncg+ cells were labeled by FG in the nondegenerating fields of both control and lasered retinas (Fig. 4B, top, respectively). Within sectors of mild degeneration in lasered retinas ( $n = 3$ ), Sncg+ cells lacking FG totaled 10% and included pNF+ RGCs of both the weak ( $3\% \pm 2\%$ ) and the strong ( $4\% \pm 3\%$ ) variety as well as Sncg+ that did not have somatic pNF ( $3\% \pm 4\%$ ; Fig. 4B, bottom left). Within sectors of severe degeneration in lasered retinas ( $n = 4$ ), the Sncg+ cells without FG totaled 85% and included pNF+ RGCs with weak and strong pNF+ ( $20\% \pm 7\%$  and  $22\% \pm 7\%$ , respectively) as well as Sncg+ cells without somatic pNF ( $43\% \pm 13\%$ ; Fig. 4B, bottom right). Irrespective



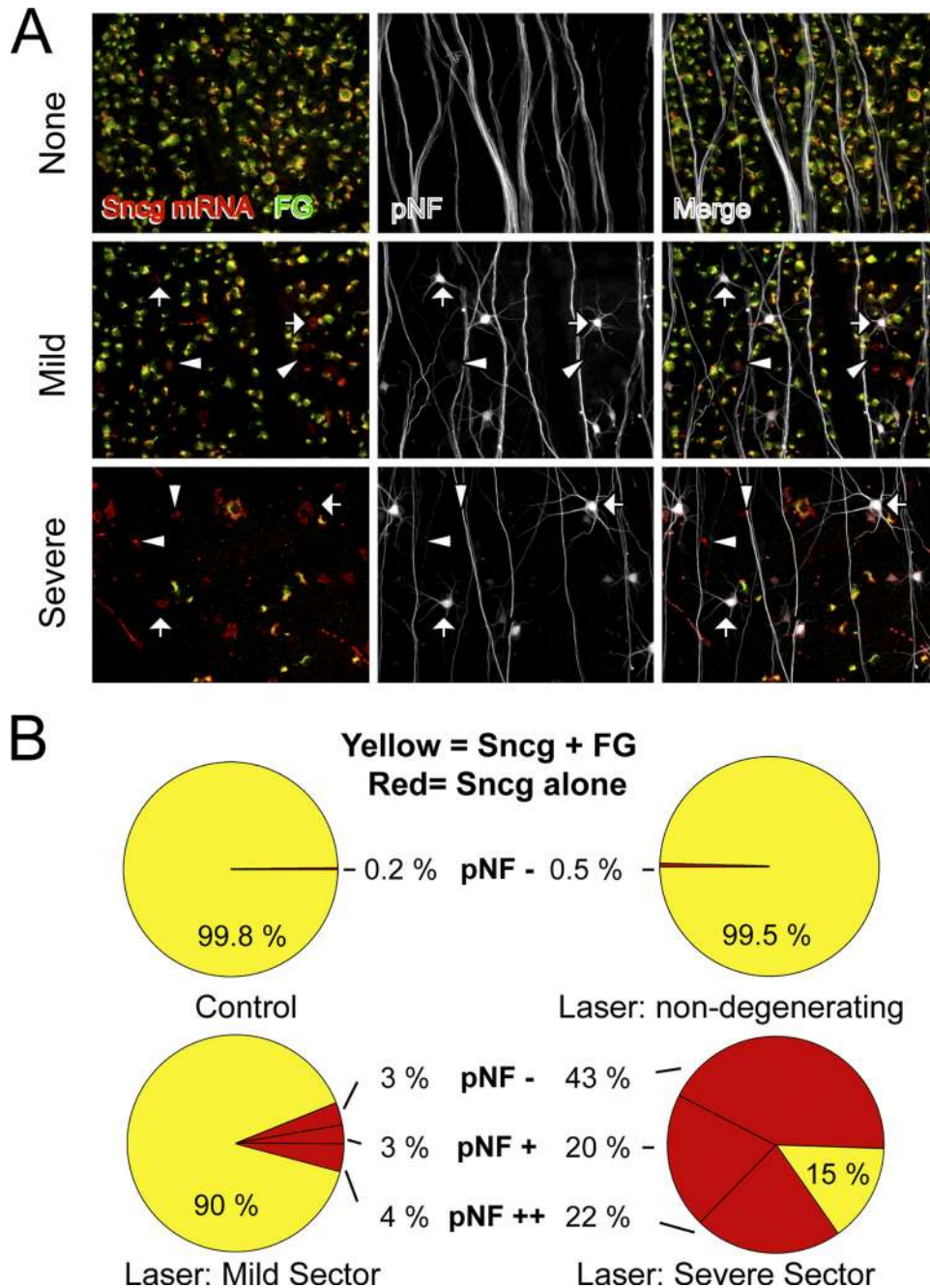


**FIGURE 4.** Sectorial degeneration involves the disconnection of RGCs. **(A)** In sectors with mild or severe degeneration within lasered retinas, there are numerous RGCs not labeled by FG, and many of these have somatic pNF (arrows) whereas others do not (arrowheads). **(B)** Based on the fraction of RGCs not labeled by FG, nondegenerating sectors within lasered retinas are indistinguishable from control retinas, but sectors with mild and severe degeneration have increased numbers of RGCs that are not labeled by FG, about half of which have somatic pNF. Nondegenerating sectors are defined as those with normal densities of Sncg+ cells and no pNF+ RGCs. Sectors with mild degeneration are defined as those with near normal densities of Sncg+ cells but with multiple nearby pNF+ RGCs. Severe degeneration sectors are defined as those with large decreases in Sncg+ cell density and numerous pNF+ RGCs. Pie charts for control, nondegenerating, mildly degenerating, and severely degenerating sectors of lasered retinas represent the mean of 4, 1, 3 and 4 retinas, respectively. Scale bar, 50  $\mu$ m.

of their locations, all pNF+ RGCs expressed Sncg mRNA, and none were labeled by FG.

### Reactive Plasticity Occurs within the Retina

We have previously reported that the intraretinal portions of RGC axons, or at least their cytoskeleton, appear to be the last part of RGCs to degenerate in DBA/2J mice.<sup>1</sup> To determine the timing of intraretinal axon degeneration in the rat translimbal laser glaucoma model, axonal labeling for pNF was analyzed in retina whole mounts at 10 and 29 days after laserling. At both time points, the extent of axonal labeling by pNF was comparable to that seen in the control retinas (Fig. 5A), even though Sncg+ cells were largely depleted from these same retinas (Fig. 2A). Indeed, in the affected retinas both at 10 days ( $n = 4$ ) and 29 days ( $n = 8$ ), the peripheral retinas had higher pNF axonal immunoreactivity

than the control retinas ( $n = 7$ ). However, axons that remained within the lasered retinas were far from normal. In particular, in the retinas 29 days after laserling, many axons were thickened, defasciculated from axon bundles, and had prominent turns and loops indicative of reactive plasticity. These abnormal profiles were most common near the optic disc (Fig. 5B). However, dystrophic processes were also found in the mid-periphery, particularly near pNF+ RGCs. Here were pNF+ neurites within the nerve fiber layer and the inner plexiform layer, as well as long processes, presumed to be axons that traveled extensively and tortuously within the inner plexiform layer (Fig. 5C). Comparable extents of reactive plasticity were observed in 7 of 8 retinas examined 29 days after laserling, and the remaining retina that had far less reactive plasticity was also the retina with the smallest loss of Sncg+ cells (data not shown). Of the

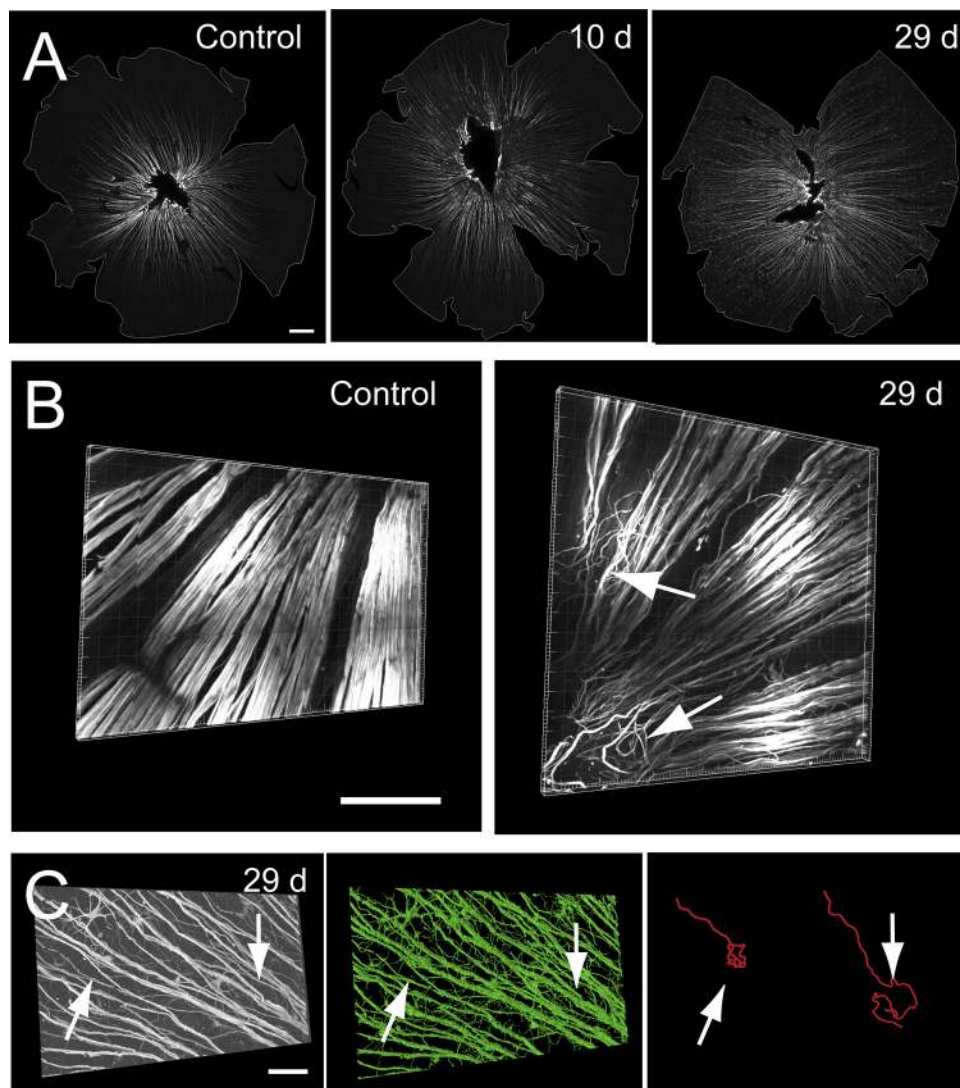


**FIGURE 5.** Persistence and reactive plasticity of intraretinal axons. (A) pNF labeling of the same retinas shown in Figure 2A showing the preservation of intraretinal axons after RGC somas are no longer detectable by Sncg mRNA. (B) Confocal stacks of axons show the presence of large numbers of axons turning near the optic disc 29 days after lasering. (C) Confocal stack of a region of midperipheral retina with mild RGC degeneration shows the presence of numerous pNF-labeled neurites from pNF+ RGCs and examples of processes coursing long distances and making turns and even knots, hallmarks of reactive plasticity. Arrows: positions of two processes presumed to be axons. Scale bars: 1 mm (A); 100  $\mu$ m (B, C).

four retinas examined 10 days after lasering, three had dystrophies of similar appearance but were much milder, and one was indistinguishable from the control retinas.

### Loss of FG Retrograde Labeling Is Largely due to the Loss of Axons in the Optic Nerve

The presence of large numbers of pNF+ RGCs and other Sncg+ cells that cannot be retrogradely labeled suggests that many RGCs remain in the retina after the optic nerve portions of their axons are damaged. Such a loss of retrograde transport could be attributed either to a severe impairment in the retrograde transport machinery or, alternatively, to physical disconnection of the axons. To distinguish between these two possibilities, optic nerves were analyzed in thin plastic sections. The optic nerves of lasered eyes had far fewer axons and numerous myelin profiles indicative of axonal degeneration at 10 days and at 29 days after the onset of IOP elevation (Fig. 6A). To estimate the extent and the time course of axon loss within the optic nerve, axons were counted at high magnification (100 $\times$  objective), identifying myelinated axons based as small objects of a lighter center and a darker surround. A new method to count such axons automatically was developed that is similar to a semiautomatic method previously used,<sup>9,10</sup> except that it counts all axons rather than just a subset and does not involve manual editing of misidentified axons. To validate

the new method, 30 sample nerves were counted with both methods, with good agreement between the two (Fig. 6B). The automatic method also enables easy identification of nerves with sectorial degeneration patterns (Fig. 6C) that can otherwise be determined only by careful inspection of high-power views of stained nerves (Supplementary Fig. S1, <http://www.iovs.org/lookup/suppl/doi:10.1167/iovs.10-5856/-DCSupplemental>). Using this automatic method,  $99,263 \pm 6,687$  axons were found in control nerves ( $n = 7$ ), and axons counts at 10 and 29 days were  $27,499 \pm 4,270$  ( $n = 4$  nerves) and  $25,905 \pm 7,282$  ( $n = 8$  nerves), respectively (Fig. 6). Thus, this model of ocular hypertension produces a significant loss of axons within the optic nerve ( $P < 0.0001$ , one-way ANOVA) that can be sectorial and that occurs largely by 10 days ( $P < 0.001$ ).

### DISCUSSION

These data are consistent with previous studies using FG labeling and Brn3A (POU4F1) antibodies to label RGCs in rat<sup>12</sup> and together suggest that most rat RGCs project primarily or by collaterals to the superior colliculus. Brn3 antibodies and Sncg mRNA probes have a significant advantage over retrograde tracers such as FG, which can grossly underestimate RGC number in optic nerve injuries such as glaucoma because of their dependence on intact axon structure between the brain



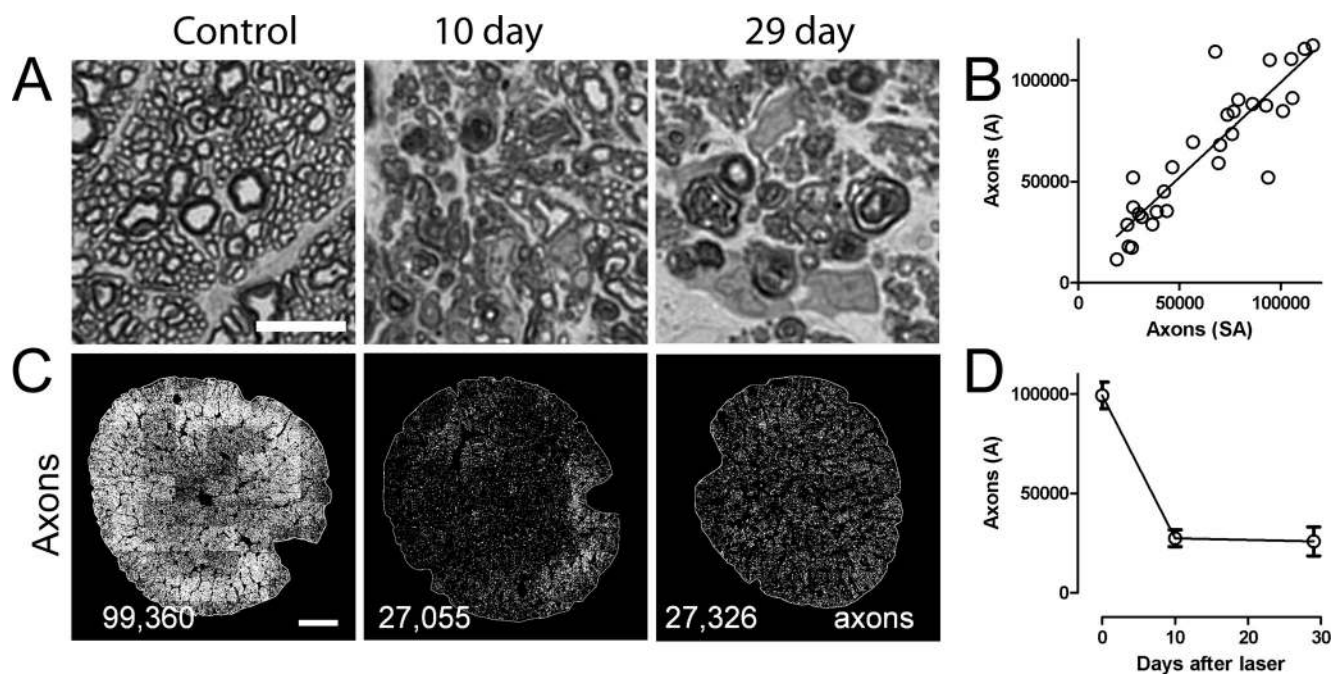


**FIGURE 6.** Axon degeneration within the optic nerve is already extensive 10 days after lasering. **(A)** Semithin plastic sections of optic nerve stained with toluidine blue reveal extensive axon loss and dystrophy by 10 and 29 days after lasering. **(B)** Novel automatic (A) axon-counting script finds similar axon numbers as an established semiautomatic (SA) axon-counting method in 30 nerves ( $P < 0.0001$ ;  $R^2 = 0.79$ ). **(C)** Novel script also produces digitized images of optic nerves that reveal local areas of high axon density, as shown in the nerve at 10 days. Unprocessed nerve images are shown in Supplementary Figure S1, <http://www.iovs.org/lookup/suppl/doi:10.1167/iovs.10-5856/-DCSupplemental>. **(D)** Axon loss is already extensive by 10 days after lasering. Scale bars: 5  $\mu\text{m}$  (A); 100  $\mu\text{m}$  (C).

and the eye. Alternatively, prelabeling RGCs before degeneration is prone to overestimate RGC numbers as the tracers are taken up by microglia that phagocytose dead RGCs.<sup>1,13</sup> A potential limitation of the use of both *Brn3a* and *Sncg* mRNA for identifying RGCs is that some RGCs may decrease their gene expression below detection limits. However, pNF+ RGCs and other nearby RGCs cannot be labeled by FG but still can be identified as RGCs based on *Sncg* mRNA expression. Thus, *Sncg* mRNA can identify RGCs even after they are severely injured.

The purpose of these studies was to determine whether three features of RGC degeneration observed in DBA/2J mice<sup>1</sup> were model specific or, rather, represented general features of glaucomatous degeneration. First, the degeneration was sectorial. Second, in and near sectors with RGC degeneration, many RGCs maintained RGC gene expression but could not be labeled retrogradely. Third, many of the RGCs that could not be retrogradely labeled had phosphorylated neurofilaments in their soma, a feature observed in other neurodegenerative disorders, such as the neurofibrillary tangles of Alzheimer's disease.<sup>14</sup>

Translimbal laser IOP elevation in the rat produces a topographic pattern of degeneration similar to that reported in DBA/2J mice<sup>1,15-18</sup>; the retinas of lasered eyes have pie-shaped sectors of RGC loss that span from the optic disc to the periphery of the retina. Sectorial degeneration patterns were observed in all lasered retinas except those with near complete loss of RGCs. This sectorial pattern is most likely explained by a focal axonal insult within the optic nerve head. In the fovea-containing human and monkey retina, the patterns of sectorial RGC loss take on arcuate shapes and are concentrated at the upper and lower poles of the nerve head in an hourglass pattern.<sup>19</sup> Given the regular radial pattern of RGC axon paths in the rodent retina, the sectorial loss seen here and in DBA/2J mice is likely the phylogenetic equivalent of the pattern of

RGC loss in human glaucoma. Because rodents have a glial lamina but lack collagen plates,<sup>20</sup> something other than collagen plates must be able to mediate localized IOP-dependent damage to axons within the optic nerve head.

Compared with *Sncg* mRNA, which is present in RGC somas before and after glaucomatous injury, pNF marks RGC somas only after injury. Normally, phosphorylated neurofilaments are found in RGC axons starting approximately 200 to 1000  $\mu\text{m}$  from the somas,<sup>21</sup> consistent with their putative role in maintaining axonal caliber.<sup>22,23</sup> However, specifically after axonal trauma, pNF appears in somas and dendrites of damaged RGCs.<sup>6-8</sup> The present study confirms previous findings in DBA/2J mice that RGCs with somatic pNF are found preferentially in the degenerating sectors of damaged retina. Comparable increases in pNF+ RGCs and sectorial loss of RGCs have recently been reported in a similar ocular hypertension model in rats.<sup>24</sup> As in DBA/2J, these pNF+ RGCs represent a significant proportion of the *Sncg*+ cells that cannot be retrogradely labeled. Whether they are a stage or a subset of degenerating RGCs is unknown. The reason most of these RGCs cannot be retrogradely labeled is likely that the portions of their axons within the optic nerve have already degenerated given that the loss of axons measured in optic nerve cross-sections 10 days after lasering is already extensive. Further, pNF+ RGCs are associated with dramatic reactive plasticity at the optic nerve head and even within the retina. Such extensive reactive plasticity is typically only seen when neurons are physically disconnected from their targets. Similar reactive plasticity has been recently reported after laser-induced increases of IOP in CD1 mice.<sup>25</sup> Unfortunately, the current methods to count RGCs in the retina and axons in the optic nerve are too crude to compare numbers of axons and RGCs within individual eyes. However, on a population basis, most of the axon loss has already occurred by 10 days, whereas the loss of RGCs continues between 10 and 29 days. All these data add to a growing

body of literature<sup>1,25-27</sup> demonstrating that axons, or at least the extraocular portion of axons, degenerate before RGC somas in glaucoma.

There are two informative differences between the RGC degenerations observed in DBA/2J mice and the rat translimbal laser model. First, in DBA/2J mice, there are hundreds of pNF+ RGCs at the peak of degeneration, whereas in the translimbal laser photocoagulation rat model, pNF+ RGCs number in the thousands. This suggests that after the more acute IOP elevation, RGC degeneration is either more synchronous or faster, or both. The second difference is that after translimbal laser photocoagulation, the pNF+ RGCs tend to be either largely of the weak variety (at 10 days) or of the strong variety (at 29 days), whereas in the DBA/2J mice, there is a more even distribution of both at any one time. This difference is likely attributable to the primary IOP insult occurring more synchronously in the current model, whereas in DBA/2J the insult occurs over a more protracted period. The current results also support the view that weak and strong pNF+ RGCs represent distinct stages in the degeneration of the same cells, as previously suggested.<sup>1</sup> Given that there are more pNF+ RGCs at 10 days than at 29 days, weak pNF+ RGCs must have at least two fates: to die quickly or to become strong pNF+ RGCs. Strong pNF+ RGCs have increased expression of *Snca* mRNA and are associated with reactive plasticity; therefore, it may be that these cells find sufficient trophic support within the retina to delay their eventual demise. Another important implication of the current studies is that, because the insult that gives rise to sectorial degeneration after short IOP increases produced by translimbal laser photocoagulation is linked to increased IOP, that which gives rise to sectorial degeneration in DBA/2J mice is also likely linked to increased IOP rather than to an unrelated inflammatory process. Finally, if pNF+ RGCs are as common in human glaucomatous retinas as they are in animal models, it may be possible to develop clinical imaging techniques to exploit their large fold-increase in number to diagnose glaucoma or to monitor its progression.

### Acknowledgments

The authors thank Scott Gelman for plastic sectioning and semiautomatic axon counts.

### References

- Soto I, Oglesby E, Buckingham BP, et al. Retinal ganglion cells downregulate gene expression and lose their axons within the optic nerve head in a mouse glaucoma model. *J Neurosci*. 2008;28(2):548-561.
- Dieterich DC, Trivedi N, Engelmann R, Gundelfinger ED, Gordon-Weeks PR, Kreutz MR. Partial regeneration and long-term survival of rat retinal ganglion cells after optic nerve crush is accompanied by altered expression, phosphorylation and distribution of cytoskeletal proteins. *Eur J Neurosci*. 2002;15(9):1433-1443.
- Dräger UC, Hofbauer A. Antibodies to heavy neurofilament subunit detect a subpopulation of damaged ganglion cells in retina. *Nature*. 1984;309(5969):624-626.
- Vidal-Sanz M, Bray GM, Villegas-Perez MP, Thanos S, Aguayo AJ. Axonal regeneration and synapse formation in the superior colliculus by retinal ganglion cells in the adult rat. *J Neurosci*. 1987;7(9):2894-2909.
- Morrison JC, Moore CG, Deppmeier LM, Gold BG, Meshul CK, Johnson EC. A rat model of chronic pressure-induced optic nerve damage. *Exp Eye Res*. 1997;64(1):85-96.
- Levkovitch-Verbin H, Quigley HA, Martin KR, Valenta D, Baumrind LA, Pease ME. Translimbal laser photocoagulation to the trabecular meshwork as a model of glaucoma in rats. *Invest Ophthalmol Vis Sci*. 2002;43(2):402-410.
- WoldeMussie E, Ruiz G, Wijono M, Wheeler LA. Neuroprotection of retinal ganglion cells by brimonidine in rats with laser-induced

- chronic ocular hypertension. *Invest Ophthalmol Vis Sci*. 2001;42(12):2849-2855.
- Morrison JC, Johnson E, Cepurna WO. Rat models for glaucoma research. *Prog Brain Res*. 2008;173:285-301.
- Levkovitch-Verbin H, Quigley HA, Martin KR, Zack DJ, Pease ME, Valenta DF. A model to study differences between primary and secondary degeneration of retinal ganglion cells in rats by partial optic nerve transection. *Invest Ophthalmol Vis Sci*. 2003;44(8):3388-3393.
- Pease ME, Zack DJ, Berlinicke C, et al. Effect of CNTF on retinal ganglion cell survival in experimental glaucoma. *Invest Ophthalmol Vis Sci*. 2009;50(5):2194-2200.
- Surgucheva I, Weisman AD, Goldberg JL, Shnyra A, Surguchov A. Gamma-synuclein as a marker of retinal ganglion cells. *Mol Vis*. 2008;14:1540-1548.
- Salinas-Navarro M, Mayor-Torroglosa S, Jimenez-Lopez M, et al. A computerized analysis of the entire retinal ganglion cell population and its spatial distribution in adult rats. *Vision Res*. 2009;49(1):115-126.
- Naskar R, Wissing M, Thanos S. Detection of early neuron degeneration and accompanying microglial responses in the retina of a rat model of glaucoma. *Invest Ophthalmol Vis Sci*. 2002;43(9):2962-2968.
- Stenberger NH, Sternberger LA, Ulrich J. Aberrant neurofilament phosphorylation in Alzheimer disease. *Proc Natl Acad Sci U S A*. 1985;82(12):4274-4276.
- Danias J, Lee KC, Zamora MF, et al. Quantitative analysis of retinal ganglion cell (RGC) loss in aging DBA/2Nnia glaucomatous mice: comparison with RGC loss in aging C57/BL6 mice. *Invest Ophthalmol Vis Sci*. 2003;44(12):5151-5162.
- Filippopoulos T, Danias J, Chen B, Podos SM, Mittag TW. Topographic and morphologic analyses of retinal ganglion cell loss in old DBA/2Nnia mice. *Invest Ophthalmol Vis Sci*. 2006;47(5):1968-1974.
- Jakobs TC, Libby RT, Ben Y, John SW, Masland RH. Retinal ganglion cell degeneration is topological but not cell type specific in DBA/2J mice. *J Cell Biol*. 2005;171(2):313-325.
- Schlamp CL, Li Y, Dietz JA, Janssen KT, Nickells RW. Progressive ganglion cell loss and optic nerve degeneration in DBA/2J mice is variable and asymmetric. *BMC Neurosci*. 2006;7:66.
- Quigley HA, Addicks EM, Green WR. Optic nerve damage in human glaucoma, III: quantitative correlation of nerve fiber loss and visual field defect in glaucoma, ischemic neuropathy, papilledema, and toxic neuropathy. *Arch Ophthalmol*. 1982;100(1):135-146.
- Howell GR, Libby RT, Jakobs TC, et al. Axons of retinal ganglion cells are insulted in the optic nerve early in DBA/2J glaucoma. *J Cell Biol*. 2007;179(7):1523-1537.
- Nixon RA, Lewis SE, Dahl D, Marotta CA, Dräger UC. Early post-translational modifications of the three neurofilament subunits in mouse retinal ganglion cells: neuronal sites and time course in relation to subunit polymerization and axonal transport. *Brain Res Mol Brain Res*. 1989;5(2):93-108.
- Hoffman PN, Griffin JW, Price DL. Control of axonal caliber by neurofilament transport. *J Cell Biol*. 1984;99(2):705-714.
- Shea TB, Paskevich PA, Beermann ML. The protein phosphatase inhibitor okadaic acid increases axonal neurofilaments and neurite caliber, and decreases axonal microtubules in NB2a/d1 cells. *J Neurosci Res*. 1993;35(5):507-521.
- Salinas-Navarro M, Alarcon-Martinez L, Valiente-Soriano FJ, et al. Ocular hypertension impairs optic nerve axonal transport leading to progressive retinal ganglion cell degeneration. *Exp Eye Res*. 2010;90(1):168-183.
- Fu CT, Sretavan D. Laser-induced ocular hypertension in albino CD-1 mice. *Invest Ophthalmol Vis Sci*. 2010;51:980-990.
- Schlamp CL, Li Y, Dietz JA, Janssen KT, Nickells RW. Progressive ganglion cell loss and optic nerve degeneration in DBA/2J mice is variable and asymmetric. *BMC Neurosci*. 2006;7:66.
- Buckingham BP, Inman DM, Lambert W, et al. Progressive ganglion cell degeneration precedes neuronal loss in a mouse model of glaucoma. *J Neurosci*. 2008;28(11):2735-2744.